

A Novel Ordered Phase in $\text{SrCu}_2(\text{BO}_3)_2$ under High Pressure

Takeshi WAKI^{1*}, Koichi ARAI^{1†}, Masashi TAKIGAWA^{1‡}, Yuta SAIGA^{1,2},
 Yoshiya UWATOKO¹, Hiroshi KAGEYAMA³, and Yutaka UEDA¹

¹*Institute for Solid State Physics, The University of Tokyo, Kashiwa, Chiba 277-8581*

²*Graduate School of Science and Engineering, Saitama University, Saitama 338-8570*

³*Department of Chemistry, Graduate School of Science, Kyoto University, Kyoto 606-8502*

(Received May 2, 2007; accepted May 31, 2007; published July 10, 2007)

We report results of ^{11}B NMR and susceptibility measurements on the quasi two-dimensional frustrated dimer spin system $\text{SrCu}_2(\text{BO}_3)_2$ under high pressure. At 2.4 GPa and in a magnetic field of 7 T, NMR lines split with decreasing temperature in two steps. A gradual splitting below $T = 30$ K breaking the four-fold symmetry of magnetic response is followed by a further sudden splitting below 3.6 K. The latter indicates a magnetic phase transition, which is also marked by a kink in the susceptibility at 1.44 GPa. From the magnetic hyperfine shift data, we conclude that the low- T phase has a doubled unit cell containing two types of dimers, one in a nearly singlet state and the other with a finite magnetization down to $T = 0$.

KEYWORDS: $\text{SrCu}_2(\text{BO}_3)_2$, Shastry–Sutherland model, high pressure, NMR, phase transition
 DOI: 10.1143/JPSJ.76.073710

A variety of exotic phenomena has been discovered in the quasi two-dimensional (2D) dimer spin system $\text{SrCu}_2(\text{BO}_3)_2$.^{1,2)} It has an alternating stack of the magnetic CuBO_3 layers [Figs. 1(a) and 1(b)] and the non-magnetic Sr layers.^{3,4)} The magnetic layer containing orthogonal arrays of spin-1/2 Cu^{2+} dimers is a realization of the 2D Shastry–Sutherland model,⁵⁾

$$H = J \sum_{\text{n.n.}} \mathbf{S}_i \cdot \mathbf{S}_j + J' \sum_{\text{n.n.n.}} \mathbf{S}_i \cdot \mathbf{S}_j, \quad (1)$$

where J (J') is the intradimer (interdimer) Heisenberg exchange interaction. The ground state of this model is obvious in two limiting cases: the dimer singlet phase for $J'/J \ll 1$ and the Néel ordered phase for $J'/J \gg 1$. The dimer singlet phase is known to be stable up to $(J'/J)_c = 0.68$.^{6–8)} Various experiments have established that $\text{SrCu}_2(\text{BO}_3)_2$ has a dimer singlet ground state at ambient pressure and zero magnetic field^{1,9,10)} with the energy gap of 33 K^{11–13)} and $J'/J = 0.60–0.64$.^{14,15)}

Frustration in the Shastry–Sutherland model strongly suppresses the kinetic energy of triplets.⁶⁾ Indeed $\text{SrCu}_2(\text{BO}_3)_2$ has an extremely small width of the triplet dispersion (~ 0.2 meV^{12,13)}). Such localized nature of triplets leads to formation of various bound states of two triplets^{15,16)} as observed by Raman¹⁷⁾ and neutron¹⁸⁾ scattering. It also leads to the magnetization plateaus at 1/8, 1/4, and 1/3 of the saturated magnetization in high magnetic fields,¹⁹⁾ where triplets crystalize in commensurate superlattices due to mutual repulsion.^{20–23)}

Since J'/J in $\text{SrCu}_2(\text{BO}_3)_2$ is close to the critical value, tuning the exchange parameters, e.g., by applying pressure, might enable us to explore the phase diagram of the Shastry–Sutherland model, which is still an open issue. A plaquette singlet phase was proposed to exist between the dimer singlet and the Néel ordered phase.^{8,24)} Alternatively, instability of two-triplet bound states²⁵⁾ may lead to a spin

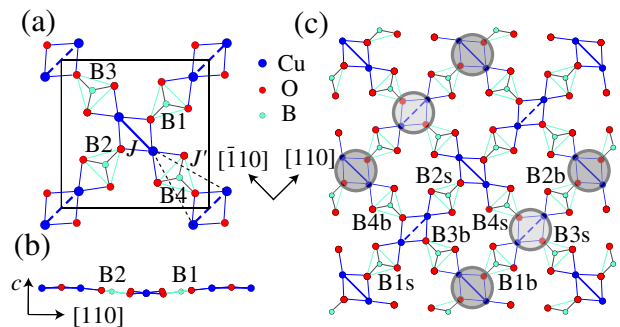


Fig. 1. (Color online) The magnetic layer of $\text{SrCu}_2(\text{BO}_3)_2$ viewed along (a) the c -direction and (b) the $[110]$ -direction. (c) A possible ordered structure in the low- T phase. Shaded circles represent the “magnetic” dimers.

nematic phase. Further variation may arise from the Dzyaloshinski–Moriya interaction beyond the Shastry–Sutherland model.²⁶⁾

In spite of such interest, only a few experiments under pressure have been reported to date. Magnetic susceptibility data up to $P = 0.7$ GPa indicates reduction of the energy gap extrapolating to zero near $P = 2.5–3.0$ GPa.²⁷⁾ The X-ray study shows a tetragonal to monoclinic structural transition at 4.7 GPa.²⁸⁾ In this letter, we report results of the nuclear magnetic resonance (NMR) experiments on ^{11}B nuclei at $P = 2.4$ GPa and the susceptibility measurements up to $P = 1.44$ GPa. Our data provide evidence for a magnetic phase transition below 4 K into an ordered phase with two distinct types of dimers.

A single crystal of $\text{SrCu}_2(\text{BO}_3)_2$ prepared by the traveling-solvent-floating-zone method²⁹⁾ was cut into a thin plate ($2.0 \times 2.8 \times 0.3$ mm³) for NMR measurements to reduce distribution of demagnetizing field. It was placed in a piston-cylinder-type pressure cell made of NiCrAl and BeCu alloys filled with 1 : 1 mixture of *N*-pentane and isoamyl-alcohol. The pressure was calibrated against the load applied at room temperature by separate measurements of the superconducting transition temperature of Sn metal. The pressure cell was

*E-mail: twac@issp.u-tokyo.ac.jp

†Present address: Hitachi Medical Corporation, Kashiwa, Chiba.

‡E-mail: masashi@issp.u-tokyo.ac.jp

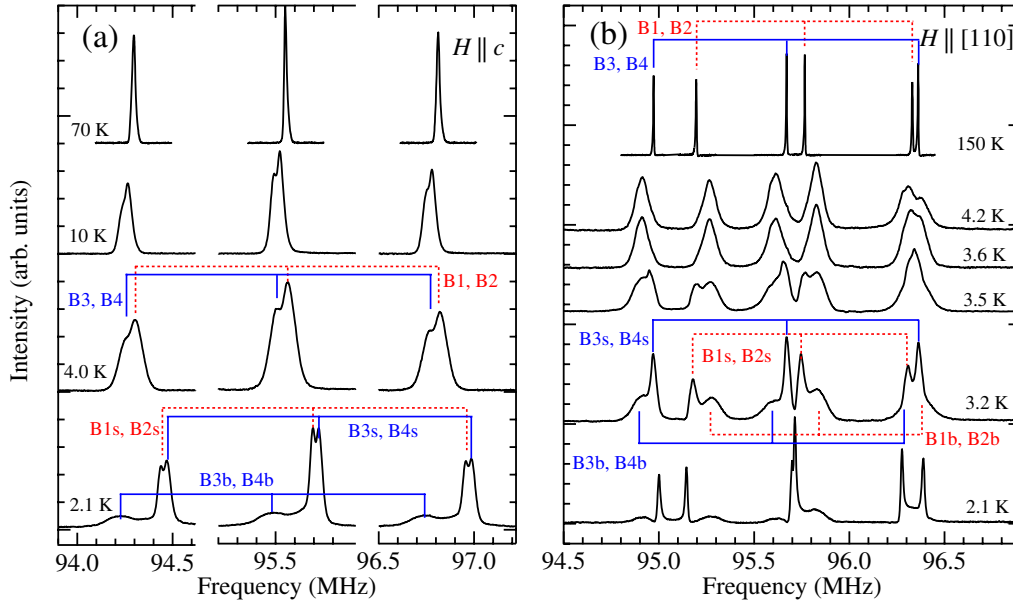


Fig. 2. (Color online) Variation of the NMR spectra with temperature at 2.4 GPa for (a) $\mathbf{H} \parallel c$ and (b) $\mathbf{H} \parallel [110]$ at the magnetic field $H = 7.006$ T. The peaks assigned to B1 and B2 (B3 and B4) are marked by the dashed (solid) lines.

mounted on the NMR probe with a double-axis-goniometer to enable arbitrary alignment of the crystal in magnetic fields. The ^{11}B NMR spectra were obtained by Fourier transforming the spin-echo signal. The demagnetizing field was corrected by comparing the NMR frequencies at ambient pressure to the published data obtained on a nearly spherical crystal.^{10,26} The susceptibility was measured on a different crystal with a SQUID magnetometer (Quantum Design, MPMS) equipped with a BeCu pressure cell³⁰ using Daphne Oil 7373 as the pressure transmitting fluid.

Figure 2 shows the NMR spectra under pressure ($P = 2.4$ GPa) at various temperatures (T) in the field $H = 7.006$ T applied along (a) the c - and (b) the $[110]$ -directions. As ^{11}B nuclei have spin $3/2$, frequencies of the quadrupole-split three NMR lines are given as,³¹⁾

$$\nu_{m \leftrightarrow m-1} = (1 + K)\gamma H + (m - 1/2)\nu_Q + \delta\nu_m^{(2)}, \quad (2)$$

$m = 3/2, 1/2,$ or $-1/2$. Here $\gamma = 13.66$ MHz/T is the nuclear gyromagnetic ratio and K is the magnetic hyperfine shift caused by the coupling between nuclei and magnetization on neighboring Cu sites. The second term is the first order quadrupole shift with ν_Q proportional to the electric field gradient (EFG) along the magnetic field direction. This term vanishes for the central line ($m = 1/2$). The third term, the second order quadrupole shift, is identical for the two satellite lines ($m = 3/2$ and $-1/2$).

$\text{SrCu}_2(\text{BO}_3)_2$ has tetragonal structure with the space group $\bar{4}2m$ at ambient pressure and temperatures below 395 K.^{3,4} The Cu and B atoms both occupy a unique $8i$ site located on the (110) or $(\bar{1}10)$ mirror plane [Fig. 1(a)]. A unit cell contains two magnetic CuBO_3 layers related by the translation $t(1/2, 1/2, 1/2)$. The four B atoms in a unit cell per layer, B1–B4 in Fig. 1(a), give distinct NMR frequencies for general field directions. The number of NMR lines is reduced for symmetric directions. When the field \mathbf{H} is in the $(\bar{1}10)$ mirror plane containing the c - and the $[110]$ -directions, B3 and B4 sites are equivalent but B1 and B2 are not due

to buckling of CuBO_3 layers [Fig. 1(b)].²⁶⁾ Then B1, B2 and (B3, B4) give three sets of quadrupole split three lines. For $\mathbf{H} \parallel [110]$, B1 and B2 also become equivalent resulting in two sets of lines. For $\mathbf{H} \parallel c$, all four sites are equivalent. The NMR spectra at ambient pressure are indeed consistent with these predictions at all temperatures.^{10,26)}

At $P = 2.4$ GPa, only one set of NMR lines is observed at high temperatures for $\mathbf{H} \parallel c$ [Fig. 2(a)], consistent with the crystal symmetry at ambient pressure. Upon cooling below 30 K, however, each line begins to split gradually and gets broadened. All three quadrupole split lines show clear double peak structure at 10 and 4 K [Fig. 2(a)]. In order to make site assignment for the split peaks, we examined variation of the spectra with the field rotated in the $(\bar{1}10)$ -plane at 10 K. We found that one of the split peaks further splits into two lines, while the other peak remains unsplit. The unsplit peak was then assigned to (B3, B4) and each of the split lines to B1 or B2. We repeated the measurements for the field rotated in the (110) -plane. The lines assigned to B3 and B4 split but lines from B1 and B2 do not, as expected.

The value of ν_Q determined from the spacing between the two satellite lines is plotted against the angle θ between \mathbf{H} and the c -direction in Fig. 3(c) for $\mathbf{H} \parallel (\bar{1}10)$ and in Fig. 3(d) for $\mathbf{H} \parallel (110)$. The θ -dependence of K is then determined from the average frequency of the two satellite lines after subtracting $\delta\nu_m^{(2)}$ calculated from the $\nu_Q(\theta)$ data³²⁾ as shown in Figs. 3(a) and 3(b).

The distinction between (B1, B2) and (B3, B4) revealed by the line splitting for $\mathbf{H} \parallel c$ must be ascribed to the loss of four fold symmetry ($\bar{4}$) around the c -direction. This symmetry requires that $\nu_Q(\theta)$ and $K(\theta)$ at B1 and B2 (B3 and B4) for $\mathbf{H} \parallel (110)$ be identical to those at B3 and B4 (B1 and B2) for $\mathbf{H} \parallel (110)$. The data in Fig. 3 show that this condition is grossly violated for the magnetic shift K but not for the quadrupole coupling ν_Q . This strongly suggests that the symmetry change is primarily due to magnetic origin

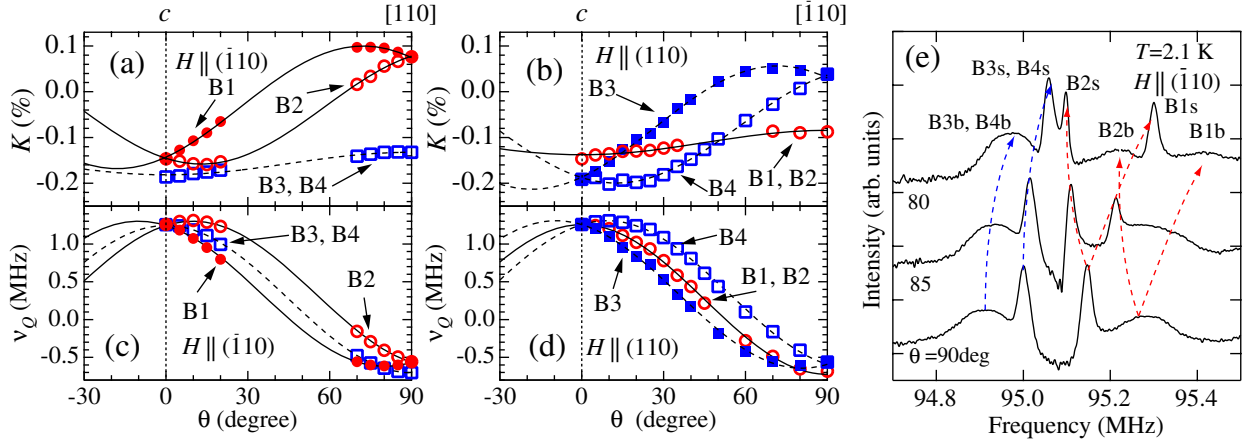


Fig. 3. (Color online) (a)–(d) Angle dependences of K and ν_Q at $T = 10$ K. The lines show the fitting explained in the text. (e) Angular variation of the NMR spectrum at $T = 2.1$ K with the field in the $(\bar{1}10)$ -plane. Only the low frequency satellite lines ($m = -1/2$) are displayed for clarity. Intensity is plotted in a logarithmic scale to make the broad lines clearly visible.

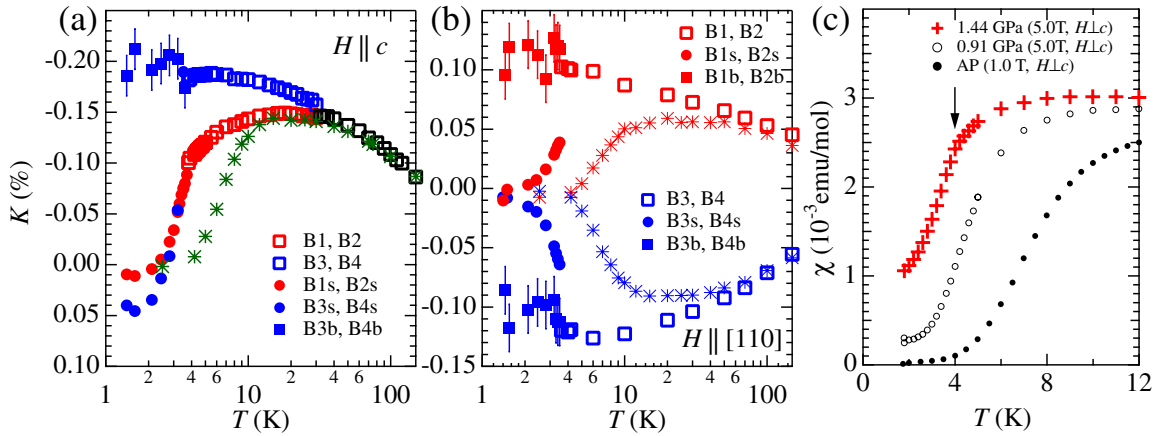


Fig. 4. (Color online) T -dependences of the shifts at 2.4 GPa for (a) $\mathbf{H} \parallel \mathbf{c}$ and (b) $\mathbf{H} \parallel [110]$ compared with the data at ambient pressure shown by crosses. (c) T -dependence of the susceptibility at ambient pressure (AP), 0.91 and 1.44 GPa.

since any structural change should be better sensed by ν_Q . Thus we conclude that the two sublattices of orthogonal Cu dimers shown by the solid and dashed lines in Fig. 1(a) become inequivalent with different magnetizations. We expect though this may accompany a slight structural change. Detailed structural analysis is left for future studies.

The $K(\theta)$ and $\nu_Q(\theta)$ data can be fit to the standard formula for anisotropic shifts, $u + v \cos^2(\theta - \alpha)$ with u , v , and α being the fitting parameters,³¹ as shown by the lines in Figs. 3(a)–3(d). We found that $K(\theta)$ and $\nu_Q(\theta)$ at B1 for $\mathbf{H} \parallel (\bar{1}10)$ [at B3 for $\mathbf{H} \parallel (110)$] are identical to $K(-\theta)$ and $\nu_Q(-\theta)$ at B2 (at B4). Thus the mirror symmetries are preserved. The loss of 4 changes the space group from $I42m$ to orthorhombic $Fmm2$. Our data indicate that the entire crystal forms a single domain.

We now discuss the NMR spectra in Fig. 2 at lower temperatures. For $\mathbf{H} \parallel [110]$, (B1, B2) and (B3, B4) give distinct lines at all temperatures. No line splitting is observed down to 3.6 K. At 3.5 K, however, all lines develop clear two peak structure. With further decreasing temperature, these two peaks change into one sharp and one broad lines with nearly equal intensity denoted as Bns and Bnb

($n = 1-4$) in Fig. 2(b). Figure 3(e) shows the variation of the low frequency satellite lines ($m = -1/2$) when the field is rotated from $[110]$ toward the c -direction at 2.1 K. Both the sharp and the broad lines from (B1, B2) split in a similar manner as observed at higher temperatures. Therefore, each of B1 and B2 must be divided into two sites below 3.6 K, (B1s, B1b) and (B2s, B2b), yielding eight inequivalent B sites for general field directions. A similar spectrum with sharp and broad lines is observed also for $\mathbf{H} \parallel \mathbf{c}$ at 2.1 K [Fig. 2(a)], although there is only one set of broad lines. We found that this belongs to (B3, B4), while the broad lines from (B1, B2) overlap with the sharp lines, by extending the measurements shown in Fig. 3(e) to smaller values of θ .

Figure 4 shows the T -dependence of the shifts at various sites for (a) $\mathbf{H} \parallel \mathbf{c}$ and (b) $\mathbf{H} \parallel [110]$ compared with the data at ambient pressure.^{10,26} Above 40 K, the results at 2.4 GPa are nearly unchanged from ambient pressure. Line splitting appears for $\mathbf{H} \parallel \mathbf{c}$ below 30 K as mentioned above. In spite of a clear change of symmetry, the splitting develops gradually without sign of a phase transition. In contrast, the second splitting at 3.6 K occurs suddenly and clearly

marks a phase transition. The shifts for the sharp lines approach near zero as $T \rightarrow 0$, pointing to a singlet ground state. We can indeed fit the data to an activation law, $\alpha + \beta \exp(-\Delta/T)$, yielding $\Delta = 11\text{--}15$ K. These values are much smaller than the gap at ambient pressure (24 K) at the same field of 7 T. The shifts for the broad lines, on the other hand, maintain large values down to the lowest temperature, pointing to a magnetic state without an excitation gap.

These results indicate coexistence of “magnetic” and “non-magnetic” Cu dimers in the low- T phase. The sharp (broad) lines should come from those B sites which couple dominantly to the non-magnetic (magnetic) Cu dimers. Preliminary results at different fields show that both the hyperfine field (K multiplied by H) and the line width for the broad lines are approximately proportional to the field, indicating no spontaneous moment at zero-field. The increased number of NMR lines indicates doubling of the primitive unit cell in the low- T phase. It is most likely that each of the Cu dimer sublattices develop spatial order of magnetic and non-magnetic dimers, forming either a superstructure in the ab -plane [see Fig. 1(c) for an example] or alternating magnetic and non-magnetic layers along the c -direction.

The susceptibility data are presented in Fig. 4(c). While no anomaly is observed at ambient pressure and at 0.91 GPa, the data at 1.44 GPa show a clear kink at 4.0 K, providing further evidence for bulk nature of the phase transition. The slightly different transition temperature is presumably due to the difference in magnetic field. Note that the susceptibility approaches a finite value as $T \rightarrow 0$ consistent with the coexistence of two types of Cu sites.

What is the order parameter describing the low- T phase? Since the magnetic dimers appears to have no spontaneous moment at zero-field but larger susceptibility than the non-magnetic dimers, a natural candidate would be the staggered component of the two-spin correlation $\langle \mathbf{S}_1 \cdot \mathbf{S}_2 \rangle$ within a dimer. This is invariant under time-reversal and considered a bond-nematic order parameter. Recently, a bond-nematic order has been proposed for frustrated spin systems on a square lattice as a result of Bose condensation of two-magnon bound states.³³ Whether such a scenario is relevant for $\text{SrCu}_2(\text{BO}_3)_2$ is an interesting issue.

To conclude, we have demonstrated that $\text{SrCu}_2(\text{BO}_3)_2$ under pressure exhibits symmetry lowering in two steps. A gradual loss of four-fold symmetry near 30 K is followed by a clear phase transition below 4 K. We propose that the low- T phase has spatial order of two types of dimers: one is nearly in a singlet state while the other has a finite susceptibility down to $T = 0$.

We thank S. Miyahara, F. Mila, T. Momoi and M. Oshikawa for stimulating discussions and T. Matsumoto for help in designing the pressure cell. This work was supported by a Grant-in-Aid for COE Research (No. 12CE2004) from the Ministry of Education, Culture, Sports, Science and Technology of Japan.

- 1) H. Kageyama, K. Yoshimura, R. Stern, N. V. Mushnikov, K. Onizuka, M. Kato, K. Kosuge, C. P. Slichter, T. Goto, and Y. Ueda: *Phys. Rev. Lett.* **82** (1999) 3168.
- 2) For a review, see S. Miyahara and K. Ueda: *J. Phys.: Condens. Matter* **15** (2003) R327.
- 3) R. W. Smith and D. A. Keszler: *J. Solid State Chem.* **93** (1991) 430.
- 4) K. Sparta, G. J. Redhammer, P. Roussel, G. Heger, G. Roth, P. Lemmens, A. Ionescu, M. Grove, G. Güntherodt, F. Hüning, H. Lueken, H. Kageyama, K. Onizuka, and Y. Ueda: *Eur. Phys. J. B* **19** (2001) 507.
- 5) B. S. Shastry and B. Sutherland: *Physica B* **108** (1981) 1069.
- 6) S. Miyahara and K. Ueda: *Phys. Rev. Lett.* **82** (1999) 3701.
- 7) Z. Weihong, C. J. Hamer, and J. Oitmaa: *Phys. Rev. B* **60** (1999) 6608.
- 8) A. Koga and N. Kawakami: *Phys. Rev. Lett.* **84** (2000) 4461.
- 9) H. Kageyama, H. Suzuki, M. Nohara, K. Onizuka, H. Takagi, and Y. Ueda: *Physica B* **281–282** (2000) 667.
- 10) K. Kodama, J. Yamazaki, M. Takigawa, H. Kageyama, K. Onizuka, and Y. Ueda: *J. Phys.: Condens. Matter* **14** (2002) L319.
- 11) H. Nojiri, H. Kageyama, Y. Ueda, and M. Motokawa: *J. Phys. Soc. Jpn.* **72** (2003) 3243.
- 12) K. Kakurai, N. Aso, K. Nukui, H. Kageyama, Y. Ueda, H. Kadowaki, and O. Cépas: in *Proc. French–Japanese Symp. Quantum Properties of Low-Dimensional Antiferromagnets*, ed. Y. Ajiro and J. P. Boucher (Kyushu University Press, Fukuoka, 2002) p. 102.
- 13) B. D. Gaulin, S. H. Lee, S. Haravifard, J. P. Castellan, A. J. Berlinsky, H. A. Dabkowska, Y. Qiu, and J. R. Copley: *Phys. Rev. Lett.* **93** (2004) 267202.
- 14) S. Miyahara and K. Ueda: *Proc. Int. Workshop Magnetic Excitations in Strongly Correlated Electrons*, *J. Phys. Soc. Jpn.* **69** (2000) Suppl. B, p. 72.
- 15) C. Knetter, A. Bühler, E. Müller-Hartmann, and G. S. Uhrig: *Phys. Rev. Lett.* **85** (2000) 3958.
- 16) K. Totsuka, S. Miyahara, and K. Ueda: *Phys. Rev. Lett.* **86** (2001) 520.
- 17) P. Lemmens, M. Grove, F. Fischer, G. Güntherodt, V. N. Kotov, H. Kageyama, K. Onizuka, and Y. Ueda: *Phys. Rev. Lett.* **85** (2000) 2605.
- 18) N. Aso, H. Kageyama, K. Nukui, M. Nishi, H. Kadowaki, Y. Ueda, and K. Kakurai: *J. Phys. Soc. Jpn.* **74** (2005) 2189.
- 19) H. Kageyama, Y. Narumi, K. Kindo, K. Onizuka, Y. Ueda, and T. Goto: *J. Alloys Compd.* **317–318** (2001) 177.
- 20) K. Kodama, M. Takigawa, M. Horvatić, C. Berthier, H. Kageyama, Y. Ueda, S. Miyahara, F. Becca, and F. Mila: *Science* **298** (2002) 395.
- 21) S. Miyahara, F. Becca, and F. Mila: *Phys. Rev. B* **68** (2003) 024401.
- 22) M. Takigawa, K. Kodama, M. Horvatić, C. Berthier, H. Kageyama, Y. Ueda, S. Miyahara, F. Becca, and F. Mila: *Physica B* **346–347** (2004) 27.
- 23) M. Takigawa, K. Kodama, M. Horvatić, C. Berthier, S. Matsubara, H. Kageyama, Y. Ueda, S. Miyahara, and F. Mila: *J. Phys.: Conf. Ser.* **51** (2006) 23.
- 24) A. Koga: *J. Phys. Soc. Jpn.* **69** (2000) 3509.
- 25) T. Momoi and K. Totsuka: *Phys. Rev. B* **62** (2000) 15067.
- 26) K. Kodama, S. Miyahara, M. Takigawa, M. Horvatić, C. Berthier, F. Mila, H. Kageyama, and Y. Ueda: *J. Phys.: Condens. Matter* **17** (2005) L61.
- 27) H. Kageyama, N. V. Mushnikov, M. Yamada, T. Goto, and Y. Ueda: *Physica B* **329–333** (2003) 1020.
- 28) I. Loa, F. X. Zhang, K. Syassen, P. Lemmens, W. Crichton, H. Kageyama, and Y. Ueda: *Physica B* **359–361** (2005) 980.
- 29) H. Kageyama, K. Onizuka, T. Yamauchi, and Y. Ueda: *J. Cryst. Growth* **206** (1999) 65.
- 30) Y. Uwatoko, T. Fujiwara, M. Hedo, F. Tomioka, and I. Umehara: *J. Phys.: Condens. Matter* **17** (2005) S1011.
- 31) C. P. Slichter: *Principles of Magnetic Resonance* (Springer, Berlin, 1989) 3rd ed.
- 32) G. H. Stauss: *J. Chem. Phys.* **40** (1964) 1988.
- 33) N. Shannon, T. Momoi, and P. Sindzingre: *Phys. Rev. Lett.* **96** (2006) 027213.